

# Genetic Manipulation of the Odor-Evoked Distributed Neural Activity in the *Drosophila* Mushroom Body

Yalin Wang,\*<sup>||</sup> Nicholas J. D. Wright,\*<sup>||</sup>#  
Hui-Fu Guo,\* Zuoping Xie,<sup>†</sup> Karel Svoboda,\*  
Roberto Malinow,\* Dean P. Smith,<sup>‡</sup> and Yi Zhong\*<sup>§</sup>

\*Cold Spring Harbor Lab

1 Bungtown Road

Cold Spring Harbor, New York 11724

<sup>†</sup>Department of Biological Sciences and

Biotechnology

Tsinghua University

Beijing

China

<sup>‡</sup>Department of Pharmacology

University of Texas Southwestern Medical Center

Dallas, Texas 75235

## Summary

Odor-induced neural activity was recorded by  $\text{Ca}^{2+}$  imaging in the cell body region of the *Drosophila* mushroom body (MB), which is the second relay of the olfactory central nervous system. The signals recorded are mainly from the cell layers on the brain surface because of the limited penetration of  $\text{Ca}^{2+}$ -sensitive dyes. The densely packed cell bodies and their accessibility allow visualization of odor-induced population neural activity. It is revealed that odors evoke diffused neural activities in the MB. Although the signals cannot be attributed to individual neurons, patterns of the population neural activity can be analyzed. The activity pattern, but not the amplitude, of an odor-induced population response is specific for the chemical identity of an odor and its concentration. The distribution pattern of neural activity can be altered specifically by genetic manipulation of an odor binding protein and this alteration is closely associated with a behavioral defect of odor preference. These results suggest that the spatial pattern of the distributed neural activity may contribute to coding of odor information at the second relay of the olfactory system.

## Introduction

Studies from both invertebrates, including *Drosophila*, and vertebrates are beginning to converge on some common mechanisms for olfactory information processing in the peripheral olfactory pathway across species (Hildebrand and Shepherd, 1997). The initial odor recognition is mediated by olfactory receptors (OR; Malnic et al., 1999) in the olfactory receptor neuron (ORN), possibly with the assistance of olfactory binding proteins (OBP; Pelosi, 1994). ORs are encoded by a large family of genes (Buck and Axel, 1991; Vosshall et al., 1999; Clyne et al., 1999a) and each ORN expresses only one or a

few receptor genes (Mombaerts et al., 1996). The ORs are broadly tuned (Duchamp-Viret et al., 1999). A single OR can recognize multiple odorants and one odorant can be recognized by multiple ORs. Odor chemical identity (quality) and concentration (quantity) are encoded at the OR level by a combinatorial OR code (Malnic et al., 1999).

As ORNs expressing the same OR genes converge on specific glomeruli in the first relay of the olfactory system, the olfactory bulb in vertebrates and the antennal lobe in insects (Mombaerts et al., 1996; Gao et al., 2000), the combinatorial OR code is turned into a glomeruli activity pattern. Odor quality and quantity are subsequently encoded by distinct spatial patterns of glomeruli activation. Odor-evoked, spatially distributed glomeruli activity has been indicated by studies using electrophysiological recording (Imamura et al., 1992; Vickers et al., 1998), 2-deoxyglucose mapping (Sharp et al., 1975; Rodrigues, 1988; Distler et al., 1998), c-fos expression patterns (Guthrie and Gall, 1995) and optical recordings (Kauer et al., 1987; Cinelli et al., 1995). Recently, advancement in optical methods has allowed direct visualization of spatially distributed patterns of odor-activated glomeruli and showed each odor can be identified with a specific glomeruli activity pattern (Friedrich and Korsching, 1997; Joerges et al., 1997; Galizia et al., 1999; Rubin and Katz, 1999).

Less study has been done at the second relay (the olfactory cortex in vertebrates and the mushroom body [MB] in insects) of the olfactory system. In the cortex and MB, input neurons make divergent connections with local neurons (Biedenbach and Stevens, 1969; Haberly, 1985; Laurent et al., 1998; Strausfeld et al., 1998). It is conceivable that odors may also induce spatially distributed neuronal activity at this level. A few available functional analyses in the cortex (Sharp et al., 1977; Schoenbaum and Eichenbaum, 1995; Litaudon et al., 1997) and in the MB (Laurent and Davidowitz, 1994), as well as computational modeling (Wilson and Bower, 1988; Bower, 1990) have indicated that odors induce distributed neuronal activity. However, it is not clear whether spatial patterns of neuronal activity at this level contain any odor information. Furthermore, no optical recordings of odor-evoked activity patterns in the cortex or mushroom bodies have been reported. These concerns prompted us to consider *Drosophila* MBs as a model for studying odor coding.

MBs have been suggested to be crucial for olfactory learning (de Belle and Heisenberg, 1994; Connolly et al., 1996; Grotewiel et al., 1998). The simple structure (2500 neurons in the *Drosophila* compared to 170,000 in the honeybee MB) and densely packed cell body regions make it a suitable candidate for optical analysis of spatially distributed activities. Also, available olfactory mutants may provide tools for manipulating activity distribution patterns. Indeed, our  $\text{Ca}^{2+}$  imaging study of odor-evoked neural activity from the living fly brain shows that the distribution pattern can be uniquely identified with odor quantity and quality. Moreover, the pattern can be altered by manipulation of expression of an OBP,

<sup>§</sup>To whom correspondence should be addressed (email: zhongyi@cshl.org).

<sup>||</sup>These authors contributed equally to this study.

<sup>#</sup>Present address: Department of Biology, Station #33, Eastern New Mexico University, Portales, New Mexico 88130.

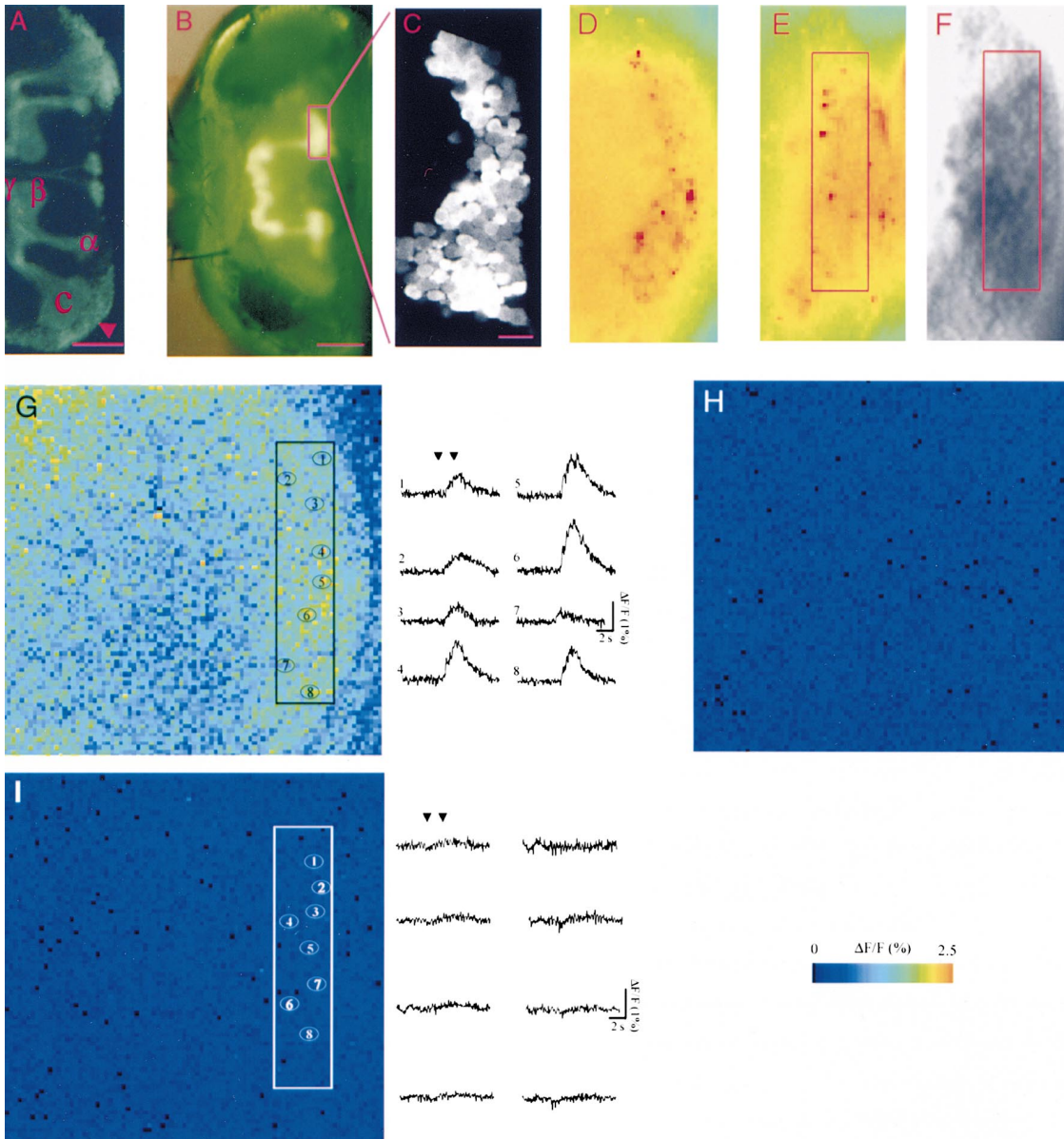


Figure 1. Odor-Induced Distributed Responses in MBs

(A) Whole mount of an isolated fly brain in which GFP is expressed in the MB. The preparation was compressed vertically to see the whole MB in one focal plane. c (calyx) is the dendritic region of the MB.  $\alpha$ ,  $\beta$ ,  $\gamma$  are three lobes of axon branches. Without compression, the  $\alpha$  lobe is pointing upward. The arrow head points to a region of densely packed MB cell bodies, which were monitored from the top in subsequent imaging studies.

(B) MBs revealed by GFP expression seen through a window cut in the head of a living fly. The fly was prepared in the same orientation as those in calcium imaging experiments.

(C) A two-photon image of the MB cell body region on the surface of the brain.

(D) The cell body region of the MB is identifiable by a high background fluorescence in a living fly loaded with Calcium Green-1.

(E and F) Background fluorescence of Calcium Green-1 (E) and  $\beta$ -Gal staining (F) of the MB of the enhancer trap line 221. The fly was first imaged for Calcium Green-1 fluorescence as in (D) and then stained for  $\beta$ -Gal expression that is shown as dense dark staining.  $\beta$ -Gal staining was aligned with the fluorescence image with the help of surrounding landmarks such as the position of residue tracheae and head bristles. The outlined regions ( $16 \times 70 \mu\text{m}$ ) contain about 70 Kenyon cell bodies on the surface and represents the area used for correlation analysis in all following figures.

(G) Left panel,  $10^{-4}$  ethyl acetate (EA)-evoked fluorescence change ( $\Delta F/F$ ) in the brain area monitored by CCD camera. The outlined rectangular region is as in (E) and (F). The right edge of the brain can be discerned as the yellow-blue boundary. Activities can be seen outside the MB cell body region. Traces on the right show the time-course of fluorescence changes from eight selected regions as marked in the left panel. Arrow heads mark the beginning and ending of the odor application (2 s).

(H) Background fluorescence change before and after the odor response.

(I) Fluorescence change when air is applied alone. Traces are time-courses of signals from the eight selected regions in the left panel.

Scale bars:  $50 \mu\text{m}$  in (A),  $100 \mu\text{m}$  in (B),  $10 \mu\text{m}$  in (C-I). Anterior is to the right and medial is to the bottom (D-I).

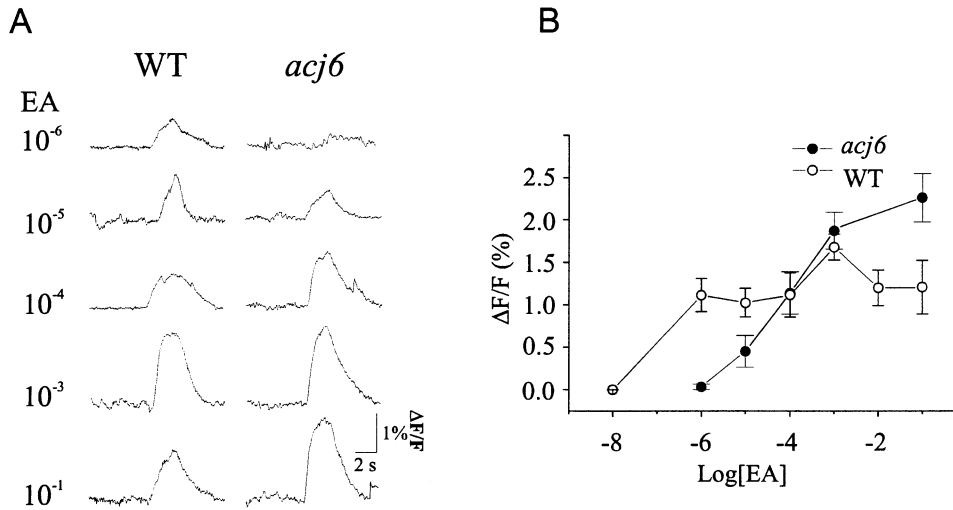


Figure 2. Altered Odor-Induced MB Activities in *acj6* Mutant Flies

(A) Time courses of  $\text{Ca}^{2+}$  signals averaged over the monitored MB region in response to stimulation by different concentrations of EA. (B) Dose response curve of activities from the monitored MB region. Data represents means  $\pm$  SEM obtained from at least five flies for each genotype.

a molecule potentially important for odor coding. This alteration of neural activity distribution is closely associated with disruption of odor preference in the OBP mutant *lush*. Our study offers the first glimpse of coding of olfactory information by population neuronal activity in the MB.

## Results

### $\text{Ca}^{2+}$ Imaging of Odor-Induced Neuronal Activities in the MBs

Targeted expression of green fluorescent protein (GFP) revealed the simple organization of MB intrinsic neurons (Kenyon cells; see Figures 1A–1C). All MB cell bodies (the area pointed by the arrow head in Figure 1A and the two-photon image in 1C) are packed densely in many layers on the surface of the dorsal side of the brain and their axons run in parallel anterior ventrally toward the central neuropil region (Figure 1A). Flies were oriented in a position that allowed direct imaging of the MB cell body region (Figure 1B). When a fly was loaded with a  $\text{Ca}^{2+}$ -sensitive dye, Calcium Green-1 or 2 (used interchangeably because no difference was found), the MB cell body region was readily identifiable because of its high fluorescence background (Figure 1D). This is further demonstrated in a fly enhancer trap line 221 that specifically expresses  $\beta$ -galactosidase ( $\beta$ -Gal) in the MB cell body region (Wright and Zhong, 1995). In this fly, the area with high Calcium Green labeling matches the  $\beta$ -Gal expression (Figures 1E and 1F).

An increase in fluorescence intensity (1%–2%) was recorded in the monitored MB region when an airborne odor, ethyl acetate (EA,  $10^{-4}$ ), was puffed onto the free-moving antennae of a living fly for 2 s (Figure 1G), indicating a  $\text{Ca}^{2+}$  influx resulted from odor-evoked electrical activity. There was no obvious drifting of the brain position as indicated by comparing background fluorescence before and after response (Figure 1H). Applying air alone did not produce any fluorescence change in the recorded brain area (Figure 1I). The odor-evoked

activity is rather diffused, with no distinct clustering. But different areas showed different amount of activity. Responses were also observed outside the MB cell body region, covering areas where the lateral horn, the MB lobes are located. This is not surprising, because many areas outside MB region in the protocerebrum receive olfactory input (Stocker et al., 1990). They were not further analyzed because we were unable to identify the structures or identity of the neurons involved. Our analyses of  $\text{Ca}^{2+}$  signal was confined in a  $16 \times 70 \mu\text{m}$  rectangular region in the MB as shown in Figure 1E and 1F, which covers about 70 Kenyon cell bodies when viewed as described previously. The responses measured by changes in the fluorescence intensity were mainly contributed by neurons in the surface area because two-photon imaging studies showed that about 81% of background fluorescence from the  $\text{Ca}^{2+}$  dyes was located in the outer  $5 \mu\text{m}$  thick cell layer. This restricted loading of  $\text{Ca}^{2+}$  sensitive dyes also suggests that the observed activity in MBs most likely reflects post-synaptic responses of MB neurons. Axon terminals of the antennal lobe projection neurons, which connect to the dendritic region (calyx in Figure 1A) of the MB, are probably too deep in the brain to be loaded with the  $\text{Ca}^{2+}$  sensitive dyes.

Increases in fluorescence intensity were specifically induced by airborne odors and depended on olfactory sensory neuron activity. This was demonstrated by the study of an olfactory mutant, *abnormal chemosensory jump 6* (*acj6*), which was isolated due to a reduced jump response to EA and other odors (McKenna et al., 1989). The *acj6* gene encodes a POU-domain transcription factor expressed in olfactory neurons (Clyne et al., 1999b). Mutations of this gene are believed to result in altered expression of odor receptors, which causes much reduced olfactory receptor potentials to odors such as EA (Ayer and Carlson, 1991; Clyne et al., 1999b). Reflected in the MB recording, the low concentration of EA ( $10^{-6}$ ) evoked responses in wild-type (WT) flies, but not in *acj6* mutants (Figure 2). Responses of  $\text{Ca}^{2+}$  activity were

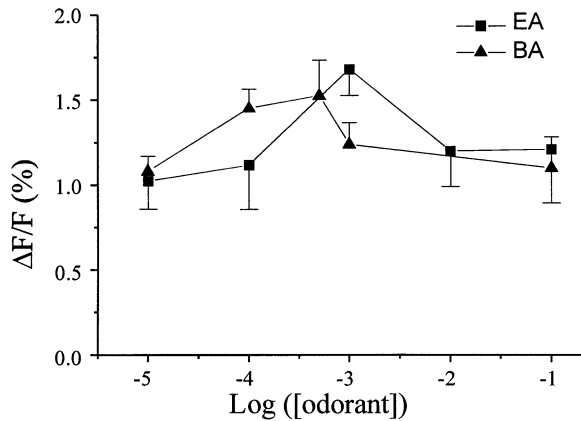


Figure 3. Dose Response Curve of Odor-Induced Activities from the Monitored MB Region of the WT Fly  
Data are presented as means  $\pm$  SEM obtained from at least five flies for each odor.

observed in the MB region of *acj6* mutants when concentrations of EA were increased to a range in which odor-induced receptor potential could be detected in antennae (Figure 2; Ayer and Carlson, 1991).

### MB Activity and Odor Representation

We then investigated how neural activities observed in MBs may change with odor quantity and quality. There seems to be no correlation between odor concentration and the amplitude of evoked population activity (Figure 3) in a broad concentration range. From  $10^{-5}$  to  $10^{-1}$ , the amount of activity in the MB evoked by EA did not change proportionally with EA concentration. A similar observation (Figure 3) was also made for responses to benzaldehyde (BA), and other odors tested (data not shown). Thus, the amplitude of the odor-induced population response in the monitored MB region does not

appear to convey information specific to odor identity or quantity.

We then compared activity patterns in the MB induced by odors. The similarity between patterns of neural activity in the defined MB region was compared pixel by pixel. A correlation coefficient,  $r$ , was calculated, which is defined as the ratio of the covariance of the sample populations to the product of their standard deviations.  $R$  is a scalar quantity in the interval of  $[-1.0, 1.0]$  ( $r = 1$  for two completely identical images;  $r = -1$  for one image is the negative of the other).

Repetitive stimulation using the same concentration of an odor induces largely reproducible activity patterns in each individual fly (Figure 4A). This is indicated by relatively high degrees of correlation ( $r = 0.62 \pm 0.04$ , see Table 1 for summaries). In contrast, different concentrations of an odor evoked quite different spatial patterns (Figures 4B, 4C) and yielded small  $r$  values (e.g.,  $0.20 \pm 0.02$  for BA; see also Table 1). Similarly, different odors tested also induced unique activity patterns (Figure 5). Such observations based on intra-individual comparisons are highly consistent from one fly to another. However, for reasons that will be discussed (see Discussion), activity patterns from different individuals were quite variable. This is evident in Figure 4. Activity patterns evoked by  $10^{-4}$  BA in Figure 4A are different from those in Figure 4B, which are obtained from a different fly. In subsequent analyses, we only compared patterns obtained within each individual preparation. Nonetheless, the quality and quantity of an odorant can be identified with a particular distribution of neural activity in the MB in each individual fly.

### Loss of Concentration-Dependent Odor Preference

To determine whether the observed distribution pattern of activity bears any significance for coding of odor information, we attempted to relate distribution patterns with a genetically altered odor-driven behavior. There are a number of mutants with defects in odor-driven

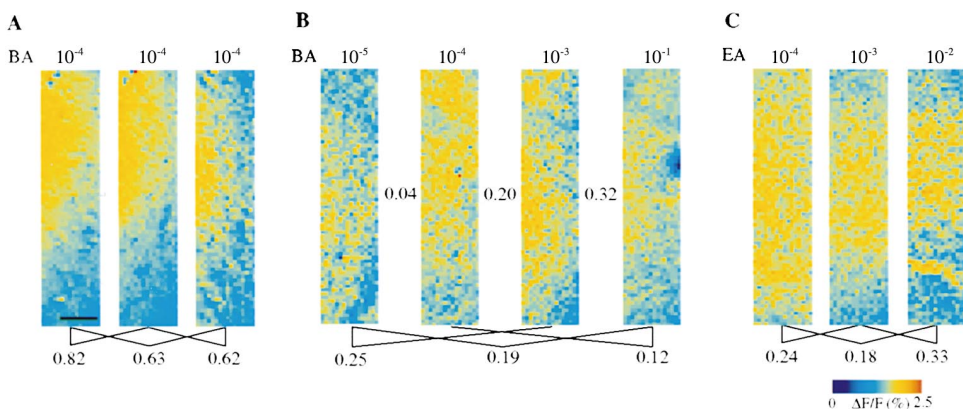


Figure 4. Spatial Representations of Odor Quantity in WT Flies

(A) Similar spatial activity patterns of calcium activity in the MB induced by the same concentration of BA. Flies were repeatedly stimulated by a 2 s application of  $10^{-4}$  BA.  
(B) Activity patterns in the MB induced by different concentrations of BA as indicated.  
(C) Activity patterns in the MB induced by different concentrations of EA as indicated. Scale bar: 10  $\mu$ m. Throughout, each group of activity patterns was obtained in a different fly. The imaging correlation coefficient  $r$  between any two of the presented patterns in each group is shown between or below the two images compared.

Table 1. Summary of Comparisons of Odor-Induced Activity Patterns in the MB

	Correlation Coefficient	Number of Comparisons Made
<b>WT</b>		
BA ( $10^{-4}$ )	$0.617 \pm 0.037$	12 (4)
BA ( $10^{-5}$ , $10^{-4}$ , $10^{-3}$ , $10^{-1}$ )	$0.196 \pm 0.023$	16 (4)
EA ( $10^{-4}$ , $10^{-3}$ , $10^{-2}$ , $10^{-1}$ )	$0.211 \pm 0.021$	22 (6)
<b>Lush</b>		
BA ( $10^{-4}$ )	$0.635 \pm 0.040$	16 (6)
BA ( $10^{-5}$ , $10^{-4}$ , $10^{-3}$ , $10^{-1}$ )	$0.652 \pm 0.030^*$	12 (3)
EA ( $10^{-4}$ , $10^{-3}$ , $10^{-2}$ )	$0.279 \pm 0.016$	12 (4)
<b>Lush Rescue</b>		
BA ( $10^{-5}$ , $10^{-4}$ , $10^{-3}$ , $10^{-1}$ )	$0.254 \pm 0.039$	18 (3)

Patterns evoked by odor stimulation of individual flies were compared, and correlation coefficients thus derived were averaged among different flies. For single odor with one concentration, comparisons were made between patterns induced by repetitive stimulations. No statistical difference at the significance level of 0.05 was found in comparisons between the mutant and the wild type except for that marked by asterisk, which showed significant difference from the wild type at 0.01 level (Student's *t* test). Data represent means  $\pm$  SEM. Numbers in parentheses represent the number of flies.

behavior (Helfand and Carlson, 1989; McKenna et al., 1989; Woodard et al., 1989; Kim et al., 1998). Among them, *lush* mutants attracted our attention because this gene encodes an OBP (Kim et al., 1998). OBPs are in-

involved in solubilizing hydrophobic odorant molecules and transporting them to receptor sites (Pelosi, 1994; Hekmat-Safe et al., 1997). They are broadly tuned to recognize odorants and may contribute to odor coding by participating in determining the chemical specificity of olfactory neurons (Kim et al., 1998). The mutant *lush* has been reported to be abnormal in avoiding ethanol in a trap assay (Kim et al., 1998). However, the trap assay requires an exposure of flies to an odorant for 2–3 days to complete a trial (Woodard et al., 1989). During this long period, many other mechanisms, such as habituation and adaptation, may influence the outcome. Therefore, the paradigm may not be suitable to study odor coding. A well-defined T-maze assay (Dudai, 1979; Tully and Quinn, 1985) was used in this study because it only requires exposing flies to odors for a short interval (2 min), which is more comparable to conditions for odor stimulation used in the optical recordings.

We first examined WT fly behavior in the T-maze in response to a number of odors, including ethanol, EA, and BA. A similar trend in response was found for all the odors tested. WT flies were attracted toward low concentrations of odors (shown in Figure 6 for EA and BA), as indicated by negative performance index (PI) scores; but were repulsed by these same odors at higher concentrations as indicated by positive PI scores. Surprisingly, the *lush* mutant flies responded normally to ethanol not only at low but also at high concentrations (data not shown). EA response was also normal in the mutant (Figure 6A). However, the mutant lost attraction specifically toward low concentrations of BA while being repulsed by high concentrations as in the WT (Figure 6B). It is noted that in the trap assay, in contrast to our finding in the T-maze assay, the *lush* mutant was normal in response to BA but abnormal to ethanol. This discrepancy may be the result of drastic differences in the duration of exposure of flies to odors in these two assays (see previous paragraph). Because of its short duration of odor exposure, the T-maze assay more likely reflects a simple olfactory response.

To ensure that the behavioral defect observed in the T-maze assay is due to the *lush* mutation, we examined

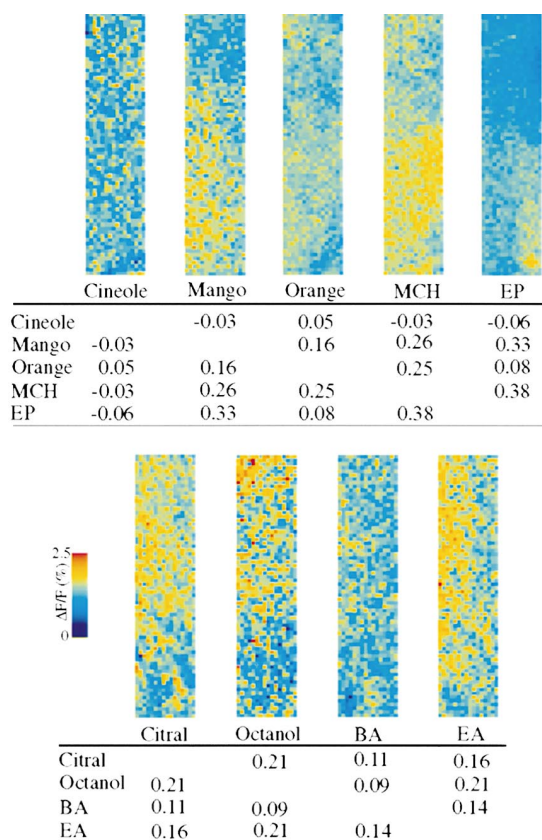


Figure 5. Spatial Representation of Odor Quality in WT Flies

The concentration for all the odors used is  $10^{-3}$ . Each odor induces a unique spatial activity pattern, as shown by the correlation coefficients listed below the images. Patterns evoked by cineole, mango, orange, 4-methyl-cyclohexanol (MCH), and ethyl propionates (EP) were from one fly and those by citral, octanol, BA, and EA were from another. Only images obtained from individual flies were compared.

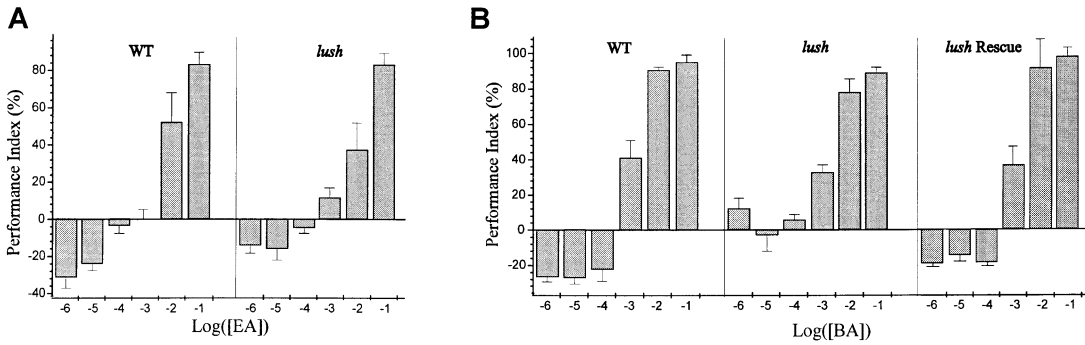


Figure 6. Altered Odor Preference in Mutant *lush* Flies

WT and *lush* flies were tested for responses to EA (A) and BA (B) in the well-established T-maze procedure as described in Experimental Procedures. Positive scores of performance index (PI) indicate repulsiveness of odors, negative scores indicate attractiveness, and 0 indicates neutral. PI = 100% or -100% represents full repulsiveness or full attractiveness, respectively. To WT flies, both EA and BA are attractive at low concentrations, but become repulsive at high concentrations. The attraction towards BA is lost in *lush* mutant flies and was rescued in the *lush* Rescue flies. At least four assays (PIs) were performed for each error bar.

the effect of expression of a cloned WT copy of *lush* (Kim et al., 1998) in the mutant background. Indeed, the behavioral defect was rescued by expression of the transgene in *lush* flies (Figure 6B). The highly specific behavioral alteration resulting from the mutation of a molecule that may be important for odor coding provided a unique opportunity to delineate the neural basis of odor coding.

#### Alteration of Neural Activity Distribution in MBs

We first examined the amplitude of BA-induced population neural activity in MBs. BA induced a similar amount of responses in both *lush* and WT flies even at low concentrations at which behavior was altered (Figure 7). This result indicated that the behavioral defect observed in the mutant was not due to its inability to sense the low concentrations of BA. A similar result was also obtained for the odorant EA (not shown). Therefore, the amplitude of population neural activity in the MB may not contribute to the behavioral defect.

We then examined the distribution of neural activity.

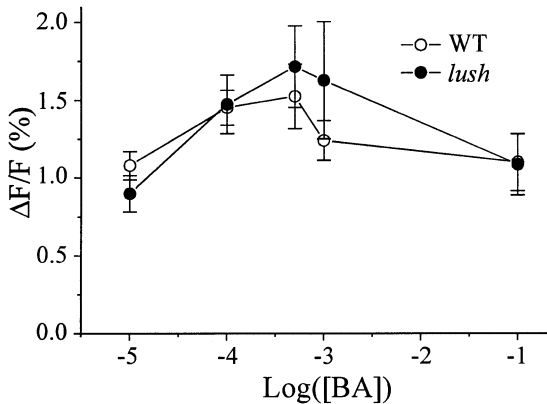


Figure 7. Dose Responses to BA in *lush* Mutant and WT Flies

Activities in the monitored MB region are measured and presented as means  $\pm$  SEM ( $n = 5$ , WT;  $n = 8$ , mutant). Only flies tested for all the shown concentrations are used for averaging. There are no significant differences between the WT and *lush* mutant flies in their overall  $Ca^{2+}$  activities evoked by BA.

Similar to WT flies, *lush* mutants showed similar activity patterns upon repetitive delivery of the same odor ( $10^{-4}$  BA; Figure 8A). The concentration-dependency of spatial distribution patterns, however, was abolished for BA in *lush* mutants. In sharp contrast to WT flies, the activity patterns induced by  $10^{-1}$ ,  $10^{-3}$ ,  $10^{-4}$ , or  $10^{-5}$  of BA (Figure 8B) were very similar to each other in *lush* mutants. A comparison of any two patterns induced by these concentrations gives rise to a much higher correlation (average  $r = 0.65 \pm 0.03$ ), which is similar to that derived from responses to the same concentration of BA (Table 1). This alteration is specific to the *lush* mutation because it was rescued by expression of a *lush* transgene (Figure 8C). In accordance with the behavioral test, the loss of the concentration-dependency of activity pattern in *lush* mutants was limited to BA among odorants tested. As in the WT, EA evoked concentration-dependent patterns of distributed neural activity in *lush* (Figure 8D). Patterns evoked by different odors, as shown by comparisons among citral, octanol, EA, and BA, also showed similar odor specificity as the WT (Figure 8E).

#### Discussion

Using  $Ca^{2+}$  imaging to monitor global neural activities, we are able to conduct the first physiological analyses of brain function in the living adult fruit fly, which has previously been extremely difficult because of its small size. The present work has focused on the MB, a second relay of olfactory central nervous system, because of the accessibility and its crucial role in olfactory related learning (de Belle and Heisenberg, 1994). We showed that optical signals recorded from the region of the MB cell bodies were specifically induced by odors through examination of a mutant fly, *acj6*. Odors at concentrations that failed to evoke receptor potentials in the sensory neurons also failed to produce any response in the MB. Then, further analysis has revealed that the distribution of neural activity changes with odor quality and concentration, while the amplitude of population activity bears no obvious correlation with odor properties. These observations suggest that odor information is represented in MBs by distributed neural activities.

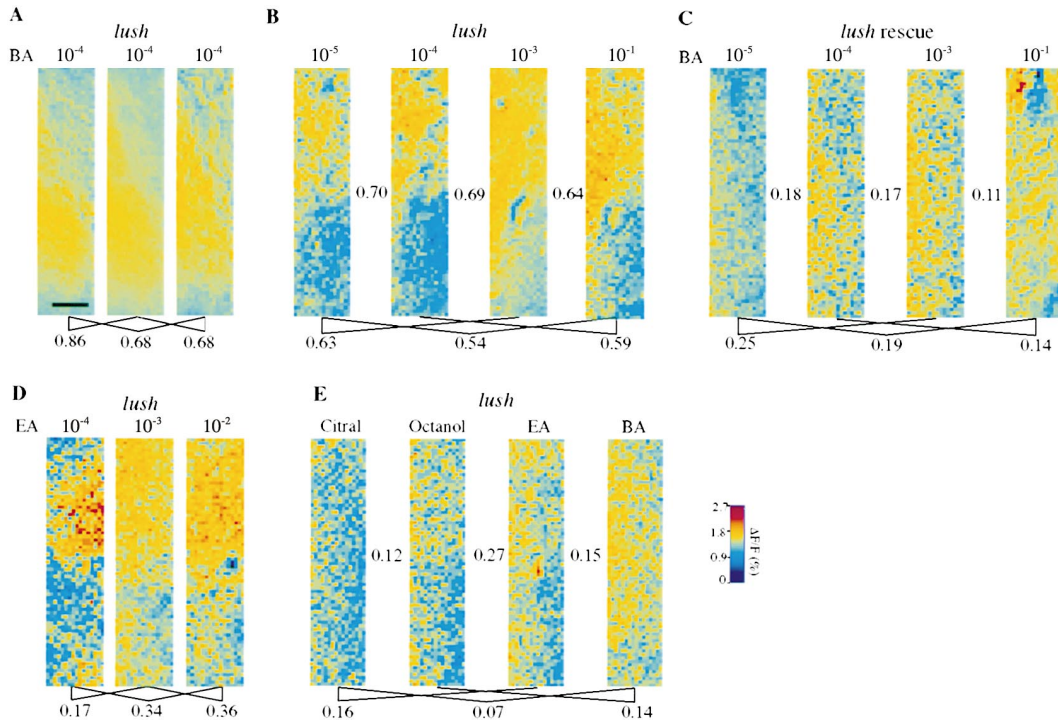


Figure 8. Alteration of Spatial Representation of BA Concentrations in *lush* Mutant Flies

Again, each group of activity patterns was obtained from a different fly. Correlations ( $r$ ) between any two responses are shown below or between the images compared.

(A) Spatial patterns of calcium activity induced by the same concentration of BA. The induced spatial activity patterns in the monitored MB region are very similar.

(B) Alteration of concentration-specificity of BA-induced spatial activity patterns in *lush* mutant flies. Correlations ( $r$ ) of patterns induced by different concentrations are similar to those of patterns induced by the same concentrations.

(C) Rescue of altered spatial representation of BA quantity by expression of a *lush* transgene.

(D) Spatial patterns in the *lush* mutant evoked by different concentrations of EA. As in the WT, different concentrations induced different patterns.

(E) Spatial activity patterns in the *lush* mutant induced by  $10^{-3}$  citral, octanol, EA, and BA. As in the WT, patterns induced by different odors are different. Scale bar, 10  $\mu\text{m}$ .

This is further supported by the study of an OBP mutant in which the loss of odor attractiveness is correlated with the alteration of the distribution of odor-evoked neural activity in MBs.

#### Ca<sup>2+</sup> Imaging in the Brain of a Living Fly

This preparation is particularly suitable for studying functions of the MB for the following reasons. First, the surface location of MB cell bodies allows easy access for dye loading and imaging. Second, its high fluorescence background after loading with Ca<sup>2+</sup> sensitive dyes makes the region of interest readily identifiable (see Figure 1D). Third, as shown in the two-photon image in Figure 1C, the densely packed soma in the MB region distribute on the brain surface rather uniformly, allowing simple comparison of activity patterns arising from a matrix of cells.

The area we monitored covers about 70 cell bodies of MB Kenyon cells. Considering that the pixel size is 1  $\mu\text{m}$  and the size of Kenyon cells is  $3.9 \pm 0.3 \mu\text{m}$  (measured from two-photon image in Figure 1C), the resolution should be enough to determine the distribution of signals to single cells. However, we are not able to relate the Ca<sup>2+</sup> activities to individual neurons because in this preparation we cannot physically identify neurons based

on Ca<sup>2+</sup>-sensitive dye fluorescence. Nevertheless, the distribution of population neuronal activity can be studied with this method.

As shown in Figures 4 and 8, it appears that activity patterns evoked by same odors are quite variable in different individuals. Comparisons of activity patterns evoked by same concentration of odors from a large pool of flies give rise to  $r$  values ranging from  $-0.43$  to  $0.51$ , mostly around  $0.1$ – $0.2$ . This variability may arise from the preparation procedure, such as the difference in dye loading and the brain orientation, and light scattering. Another possibility is that the variation reflects intrinsic individual difference at MB level. In other words, each fly may have a different neural representation for a specific odor. We could not distinguish between these two possibilities in the present time. However, results from intra-individual comparisons are highly consistent across individuals.

#### Odor Responses at the Second Relay of the Central Nervous System

This study provides a number of interesting observations comparing to those observed in peripheral sensory neurons and in the first relay of the central nervous system. First, the amplitude of population neuron activ-

ity in the observed region appeared not to vary a lot over a wide range of concentrations tested (from  $10^{-5}$  to  $10^{-1}$  dilution; see Figure 3), which implies that overall neural activity levels do not carry odor information. In contrast, electrophysiological recordings from fly ORNs have shown that higher concentrations elicit larger receptor potentials (Ayer and Carlson, 1991; Krishnan et al., 1999). In the antennal lobe, 2-deoxyglucose mapping has shown a positive correlation between odor concentration and odor response (Rodrigues, 1988). Such a relationship between amplitude of response and odor concentration is also observed in other organisms by various functional analyses including optical recordings (Cinelli et al., 1995; Friedrich and Korsching, 1997; Joerges et al., 1997; Rubin and Katz, 1999). So it seems that in the second relay of the olfactory pathway of the *Drosophila*, the part of amplitude-related odor representation at earlier stages is transformed into a distributed spatial representation.

Second, odor-evoked activities in the MB are distributed. In the antennal lobe, depending on its concentration, an odor elicits restricted response in a subset of glomeruli as shown by 2-deoxyglucose mapping in flies (Rodrigues, 1988). This is directly seen with optical imaging in the honeybee, zebrafish, and rat (Joerges et al., 1997; Friedrich and Korsching, 1997; Rubin and Katz, 1999). However, as shown in this study, odor-evoked activities in the *Drosophila* MB are rather dispersed in the whole area, stronger in some places than others. We do not see any confinement of activity to a subregion or subregions. It is known from anatomical studies that in insect olfactory input neurons make divergent contacts in the MB (Laurent et al., 1998; Strausfeld et al., 1998). It is not surprising to see in the MB distributed response to odor stimulation. In fact, it has been suggested that in the olfactory cortex odor-induced responses might be diffused and widely spread based on observations of extensive connection among input projection neurons and interneurons (Haberly, 1985).

### Distributed MB Activity Pattern and Odor Representation

In this study, we have shown that odorant quality and quantity are uniquely identified with spatial activity patterns. Moreover, the mutation of an OBP that may be important for odor coding leads to alteration of the distribution of MB neuronal activity and alteration of perceived odor quality. We hypothesize that the pattern of spatially distributed MB activity may contain odor information necessary for perception of odor attractiveness.

However, there are two issues that need to be addressed. First, the behavioral defect of the *lush* mutant is limited to low concentrations of BA, but the distribution of neuronal activity in *lush* is altered at all concentrations tested, including those at which the repulsive behavior is normal. We speculate that repulsiveness of an odor is processed in other brain regions such as the lateral horn of the protocerebrum, but not in the MB. It has been reported in humans that strong aversive odors induce neural activity in different brain regions as compared to those induced by neutral or attractive odorants (Zald and Pardo, 1997). It is possible that different quali-

ties of odors are also processed in different regions of the *Drosophila* brain. In fact, it is known that both the lateral horn and MB receive input from the antennal lobe (Stocker et al., 1990). Each unique distribution pattern of the MB activity associated with an odor contains information related to odor attractiveness but not repulsiveness regardless of concentration. Therefore, the *lush* mutant only lost attractiveness but retained normal repulsiveness, even though the distribution of activity in the MB is altered at all concentrations of BA.

The hypothesis predicts that manipulating MB activity would only alter odor attractiveness, not repulsiveness. Blocking MB activity by expressing the temperature-sensitive mutant *shibire* gene specifically abolished odor attractiveness without affecting repulsiveness (Wang et al., 2000; personal communication with Josh Dubnau and Tim Tully). This conforms that odor attractiveness is processed in the MB and provides support for our hypothesis.

Second, does this odor-specific distribution pattern of MB activity indicate a spatial coding mechanism or an identity one? The conventional concept of spatial coding often means an identity code, in which information is defined by the identities of activated neurons rather than their physical position (Laurent, 1999). To be truly spatial, the exact position of neurons has to be an intrinsic and necessary part of coding, as in the retina or cochlea, for example. By this definition, our analysis of MB activity would argue for an identity coding mechanism. Which neurons are firing rather than where they lie carries information about the odorant and concentration. However, because the current study could not relate the MB activity to each single identifiable neuron and activities between individual flies could not be compared with great confidence, addressing the variability of this code will have to await simultaneous identification of individual MB neurons and monitoring of their activity. We are currently working on such a method.

### Experimental Procedures

#### Fly Stocks

*Acj6* flies were kindly provided by Dr. John Carlson. The *acj6* is X chromosome-linked and maintained over the *C(1)A y*-attached X chromosome (McKenna et al., 1989). The *lush* mutant is as described (Kim et al., 1998).

#### Living Fly Preparation and Dye Loading

Flies were held in a truncated 25  $\mu$ l pipette tip, trimmed so that the top of the fly head was exposed. A small window was cut in the head by removing a piece of cuticle and tracheae to expose the part of the brain where calyces are located. A drop of 1  $\mu$ M Calcium Green-1 AM (Molecular Probes, Eugene, OR) in adult fly saline (Trimarchi and Murphey, 1997) (115 mM  $\text{Na}_3\text{Cl}$ , 5 mM KCl, 6 mM  $\text{CaCl}_2 \cdot 2\text{H}_2\text{O}$ , 1 mM  $\text{MgCl}_2 \cdot 6\text{H}_2\text{O}$ , 4 mM  $\text{Na}_2\text{HCO}_3$ , 1 mM  $\text{NaH}_2\text{PO}_4 \cdot \text{H}_2\text{O}$ , 5 mM trehalose, 75 mM sucrose, and 5 mM N-Tris [hydroxymethyl] methyl-2-aminoethane sulfonic acid) was placed to cover the opening for 30 min at room temperature. The Calcium Green solution was first made by dissolving 50  $\mu$ g dye in 38  $\mu$ l 20% Pluronic in DMSO and then diluting 1000-fold in fly saline. The dye solution was removed with several washes with fly saline and the window in the fly head was covered by a cover slip with a tiny window cut to match that in the head. A drop of the fly saline was placed over the cover slip to accommodate the water immersion lens.

#### $\beta$ -Gal Staining

The staining was carried out with a procedure described previously (Wright and Zhong, 1995) with some modification. Briefly, the ex-

posed fly brain was placed under a drop of 0.2% 5-bromo-4-chloro-3-indoxyl- $\beta$ -D-galactopyranoside which was freshly made in the staining buffer (10 mM NaH<sub>2</sub>PO<sub>4</sub>, 3.1 mM K<sub>4</sub>[Fe(II)(CN)<sub>6</sub>], 3.1 mM K<sub>3</sub>[Fe(III)(CN)<sub>6</sub>], 150 mM NaCl, 1 mM MgCl<sub>2</sub>) for 2 hr at room temperature. The fly was kept in a closed moist chamber to keep from drying.  $\beta$ -Gal expression is visualized as dense black staining under normal light microscope.

#### Optical Recording

An Eosin filter set was used for Calcium Green imaging, which included a HQ500/40x Exciter, Q530LP Dichroic Beamsplitter, and HQ560/50m Emitter. The light source was an OSRAM HBO Mercury Short Arc lamp. Fluorescent images (128  $\times$  128 pixel) were collected at room temperature via a water immersion lens (Olympus  $\times$ 63) and recorded (about 20 frames per second) using a cooled CCD camera (Life Science Resources, UK). Exposure time per frame was 20 ms. Recording was started about 3 s before the onset of stimulation and lasted for 12 s. Images of distributed Ca<sup>2+</sup> activity were obtained by averaging 10–20 frames at the peak of the response after subtraction of the average of a series of frames obtained without stimulus. They were false color-coded and presented as relative changes in fluorescence over the background ( $\Delta F/F$ ). For each preparation, all conditions were made constant for stimulation delivery, imaging, and data analysis.

During recording, the fly was in a constant air stream (clinical blood gas mixture, flow rate: 0.1 liter/min) bubbled through mineral oil to minimize mechanical effects. The air stream was directed at the fly by a micropipette placed about 1 cm away from fly's freely moving antennae. Odor puffs were applied by switching from the air stream to an odor stream which was produced by bubbling air through mineral oil containing an odor. Odor concentrations were determined by the volume percentage of odorant in mineral oil. For example, 10<sup>-3</sup> corresponding to a 1000-fold dilution of the pure odorant into mineral oil. The duration of odor stimulation was 2 s. To ensure that the observed response was odor-induced, a control sweep was recorded preceding the odor delivery by switching from one constant air stream to another under the same pressure. Odor stimulations were applied in a randomized order with about two-minute interval between applications.

#### Two-Photon Laser Scanning Microscope

In vivo two-Photon Laser Scanning Microscope (2PLSM) imaging was achieved using a custom-designed microscope (Svoboda et al., 1997). The excitation light was set to  $\lambda \sim 910$  nm and  $\lambda \sim 800$  nm, for GFP and Calcium Green-1 imaging, respectively. Data analysis was performed with custom software written in IDL (Research Systems).

#### Analyses

The "degree of fit" between two images was quantified by the correlation coefficient  $r$  in a linear model provided in IDL software (Research Systems, Inc.). The correlation  $r$  is defined as the ratio of the covariance of the sample populations to the product of their standard deviations, which is a scalar quantity in the interval [-1.0, 1.0] (a value of  $r$  close to 1 indicates a high degree of correlation;  $r$  close to 0 indicates poor correlation). To minimize the possible artifact caused by movement, only data from preparations that showed no visible drift of brain position were used. Data with movement were further excluded by comparing background fluorescence patterns at different times during a trial as well as from different trials to minimize the effect of the drift of brain position. We also compared frames acquired at different times within the course of the odor response to ensure that the variation of patterns is not resulted from movements. For the data used in analysis, patterns of the background level of fluorescence were almost identical at any moment within a trial ( $r = 0.995 \pm 0.001$ ) as well as among different trials ( $r = 0.94 \pm 0.01$ ) recorded from the same fly. Comparisons of the frames acquired at different times of the responses (rising phase, peak, falling phase) give rise to a  $r$  value of  $0.92 \pm 0.02$ , indicating no significant pattern change during the fly's response to odor stimulation. Images with any of such  $r$  values less than 0.9 are discarded. A small pulsing movement, probably resulted from the heart beating, was smoothed out by averaging multiple frames.

#### Behavioral Test

The apparatus and procedure have been described extensively (Tully and Quinn, 1985). Briefly, about 150 flies are loaded into the choice point of the T-maze and allowed to choose between the odor (such as EA or BA) versus air for 2 min. Flies trapped in each arm of the T-maze were counted, and a performance index (PI) was calculated for each odor individually:  $PI = ((COR - 0.5)/0.5) \times 100 = ((COR \times 2) - 1) \times 100$ . COR stands for "probability correct", which is calculated as the number of flies avoiding the odor divided by the total number of flies in the T-maze arms. A positive or a negative PI means that flies are repulsed or attracted, respectively, by an odor.

#### Acknowledgments

We thank Drs. Z. Mainen, P. O'Brien, J. Sheng for technical help in data analyses and two-photon imaging. This work was supported by a fellowship from the Henry Wendt Neuroscience Fellowships to YW and grants from NIH NS34779 and HD33098 and scholarship from Pew Foundation to YZ.

Received February 24, 2000; revised December 5, 2000.

#### References

- Ayer, R.K., and Carlson, J. (1991). *acj6*: A gene affecting olfactory physiology and behavior in *Drosophila*. Proc. Natl. Acad. Sci. USA 88, 5467–5471.
- Biedenbach, M.A., and Stevens, C.F. (1969). Synaptic organization of cat olfactory cortex as revealed by intracellular recording. J. Neurophysiol. 32, 204–214.
- Bower, J. (1990). Reverse engineering the nervous system: an anatomical, physiological, and computer based approach. In An Introduction to Neural and Electronic Networks, S.F. Zornetzer, J.L. Davis, and C. Lau, eds. (San Diego: Academic Press), p. 3.
- Buck, L.B., and Axel, R. (1991). A novel multigene family may encode odorant receptors: a molecular basis for odor recognition. Cell 65, 175–187.
- Cinelli, A.R., Hamilton, K.A., and Kauer, J.S. (1995). Salamander olfactory bulb neuronal activity observed by video rate, voltage-sensitive dye imaging. III. Spatial and temporal properties of responses evoked by odorant stimulation. J. Neurophysiol. 73, 2053–2071.
- Clyne, P.J., Warr, C.G., Freeman, M.R., Lessing, D., Kim, J., and Carlson, J.R. (1999a). A novel family of divergent seven-transmembrane protein: candidate odorant receptors in *Drosophila*. Neuron 22, 327–338.
- Clyne, P.J., Certel, S.J., de Bruyne, M., Zaslavsky, L., Johnson, W.A., and Carlson, J.R. (1999b). The odor specificities of a subset of olfactory receptor neurons are governed by Acj6, a POU-domain transcription factor. Neuron 22, 339–347.
- Connolly, J.B., Roberts, I.J.H., Armstrong, J.D., Kaiser, K., Forte, M., Tully, T., and O'Kane, C.J. (1996). Associative learning disrupted by impaired Gs signaling in *Drosophila* mushroom bodies. Science 274, 2104–2107.
- de Belle, J.S., and Heisenberg, M. (1994). Associative odor learning in *Drosophila* abolished by chemical ablation of mushroom bodies. Science 263, 692–695.
- Distler, P.G., Bausenwein, B., and Boeckh, J. (1998). Localization of odor-induced neuronal activity in the antennal lobes of the blowfly *Calliphora vicina*: a [<sup>3</sup>H] 2-deoxyglucose labeling study. Brain Res. 805, 263–266.
- Duchamp-Viret, P., Chaput, M.A., and Duchamp, A. (1999). Odor response properties of rat olfactory receptor neurons. Science 284, 2171–2174.
- Dudai, Y. (1979). Behavioral plasticity in a *Drosophila* mutant, dunce DB276. J. Comp. Physiol. 130, 271–275.
- Friedrich, R.W., and Korsching, S.I. (1997). Combinatorial and odorant coding in the zebrafish olfactory bulb visualized by optical imaging. Neuron 18, 737–752.

- Galizia, C.G., Sachse, S., Pappert, A., and Menzel, R. (1999). The glomerular code for odor representation is species specific in the honeybee *Apis mellifera*. *Nature Neurosci.* 2, 473–478.
- Gao, Q., Yuan, B., and Chess, A. (2000). Convergent projections of *Drosophila* olfactory neurons to specific glomeruli in the antennal lobe. *Nature Neurosci.* 3, 780–785.
- Grotewiel, M.S., Beck, C.D., Wu, K.H., Zhu, X.R., and Davis, R.L. (1998). Integrin-mediated short-term memory in *Drosophila*. *Nature* 391, 455–460.
- Guthrie, K.M., and Gall, C.M. (1995). Functional mapping of odor-activated neurons in the olfactory bulb. *Chem. Senses.* 20, 271–282.
- Haberly, L.B. (1985). Neuronal circuitry in olfactory cortex: anatomy and functional implications. *Chem. Senses* 10, 219–238.
- Hekmat-Scafe, D.S., Steinbrecht, R.A., and Carlson, J.R. (1997). Coexpression of two odorant-binding protein homologs in *Drosophila*: implications for olfactory coding. *J. Neurosci.* 17, 1616–1624.
- Helfand, S.L., and Carlson, J.R. (1989). Isolation and characterization of an olfactory mutant in *Drosophila* with a chemically specific defect. *Proc. Natl. Acad. Sci. USA* 86, 2908–2912.
- Hildebrand, J.G., and Shepherd, G.M. (1997). Mechanisms of olfactory discrimination: Converging evidence for common principles across phyla. *Annu. Rev. Neurosci.* 20, 595–631.
- Imamura, K., Mataga, N., and Mori, K. (1992). Coding of odor molecules by mitral/tufted cells in rabbit olfactory bulb. I. Aliphatic compounds. *J. Neurophysiol.* 68, 1986–2002.
- Joerges, J., Küttner, A., Galizia, C.G., and Menzel, R. (1997). Representations of odours and odour mixtures visualized in the honeybee brain. *Nature* 387, 285–288.
- Kauer, J.S., Senseman, D.M., and Cohen, L.B. (1987). Odor-elicited activity monitored simultaneously from 124 regions of the salamander olfactory bulb using a voltage-sensitive dye. *Brain Res.* 418, 255–261.
- Kim, M.-S., Repp, A., and Smith, D.P. (1998). LUSH odorant-binding protein mediates chemosensory responses to alcohols in *Drosophila melanogaster*. *Genet.* 150, 711–721.
- Krishnan, B., Dryer, S.E., and Hardin, P.E. (1999). Circadian rhythms in olfactory responses of *Drosophila melanogaster*. *Nature* 400, 375–378.
- Laurent, G. (1999). A systems perspective on early olfactory coding. *Science* 286, 723–728.
- Laurent, G., and Davidowitz, H. (1994). Encoding of olfactory information with oscillating neural assemblies. *Science* 265, 1872–1875.
- Laurent, G., MacLeod, K., Stopfer, M., and Wehr, M. (1998). Spatio-temporal structure of olfactory inputs to the mushroom bodies. *Learning and memory* 5, 124–132.
- Litaudon, P., Datiche, F., and Cattarelli, M. (1997). Optical recording of the rat piriform cortex activity. *Prog. Neurobiol.* 52, 485–510.
- Malnic, B., Hirono, J., Takaaki, S., and Buck, L.B. (1999). Combinatorial receptor codes for odors. *Cell* 96, 713–723.
- McKenna, M., Monte, P., Helfand, S.L., Woodard, C., and Carlson, J.R. (1989). A simple chemosensory response in *Drosophila* and the isolation of *acj* mutants in which it is affected. *Proc. Natl. Acad. Sci. USA* 86, 8118–8122.
- Mombaerts, P., Wang, F., Dulac, C., Chao, S.K., Nemes, A., Mendelsohn, M., Edmondson, J., and Axel, R. (1996). Visualizing an olfactory sensory map. *Cell* 87, 675–686.
- Pelosi, P. (1994). Odorant-binding proteins. *Critic. Rev. Biochem. Mol. Biol.* 29, 199–228.
- Rodrigues, V. (1988). Spatial coding of olfactory information in the antennal lobe of *Drosophila melanogaster*. *Brain Res.* 453, 299–307.
- Rubin, B.D., and Katz, L.C. (1999). Optical imaging of odorant representations in the mammalian olfactory bulb. *Neuron* 23, 499–511.
- Schoenbaum, G., and Eichenbaum, H. (1995). Information coding in the rodent prefrontal cortex. II. Ensemble activity in orbitofrontal cortex. *J. Neurophysiol.* 74, 751–762.
- Sharp, F.R., Kauer, J.S., and Shepherd, G.M. (1975). Local sites of activity-related glucose metabolism in rat olfactory bulb during olfactory stimulation. *Brain Res.* 98, 596–600.
- Sharp, F.R., Kauer, J.S., and Shepherd, G.M. (1977). Laminar analysis of 2-deoxyglucose uptake in olfactory bulb and olfactory cortex of rabbit and rat. *J. Neurophysiol.* 40, 800–813.
- Stocker, R.F., Lienhard, M.C., Borst, A., and Fischbach, K.-F. (1990). Neuronal architecture of the antennal lobe in *Drosophila melanogaster*. *Cell Tissue Res.* 262, 9–34.
- Strausfeld, N.J., Hansen, L., Li, Y., Gomez, R.S., and Ito, K. (1998). Evolution, discovery, and interpretations of arthropod mushroom bodies. *Learning & Memory* 5, 11–37.
- Svoboda, K., Denk, W., Kleinfeld, D., and Tank, D.W. (1997). *In vivo* dendritic calcium dynamics in neocortical pyramidal neurons. *Nature* 385, 161–165.
- Trimarchi, J.R., and Murphey, R.K. (1997). The *shaking-B2* mutation disrupts electrical synapses in a flight circuit in adult *Drosophila*. *J. Neurosci.* 17, 4700–4710.
- Tully, T., and Quinn, W.G. (1985). Classical conditioning and retention in normal and mutant *Drosophila melanogaster*. *J. Comp. Physiol.* 157, 263–277.
- Vickers, N.J., Christensen, T.A., and Hildebrand, J.G. (1998). Combinatorial odor discrimination in the brain: attractive and antagonist odor blends are represented in distinct combinations of uniquely identifiable glomeruli. *J. Comp. Neurol.* 400, 35–56.
- Vosshall, L.B., Amrein, H., Morozov, P.S., Rzhetsky, A., and Axel, R. (1999). A spatial map of olfactory receptor expression in the *Drosophila* antenna. *Cell* 96, 725–736.
- Wang, Y., Guo, H.-F., Kitamoto, T., and Zhong, Y. (2000). *Soc. Neurosci.* 30, abstract 451.7.
- Wilson, M.A., and Bower, J.M. (1988). A computer simulation of olfactory cortex with functional implications for storage and recognition of olfactory information. In *Neural Information Processing Systems*, D.Z. Anderson, ed. (New York: AIP), pp. 114–126.
- Woodard, C., Huang, T., Sun, H., Helfand, S.L., and Carlson, J.R. (1989). Genetic analysis of olfactory behavior in *Drosophila*: A new screen yields the *ota* mutants. *Genetics* 123, 315–326.
- Wright, N.J.D., and Zhong, Y. (1995). Characterization of K<sup>+</sup> currents and the cAMP-dependent modulation in cultured *Drosophila* mushroom body neurons identified by *lacZ* expression. *J. Neurosci.* 15, 1025–1034.
- Zald, D.V., and Pardo, J.V. (1997). Emotion, olfaction, and the human amygdala: Amygdala activation during aversive olfactory stimulation. *Proc. Natl. Acad. Sci. USA* 94, 4119–4124.